Analytical Biochemistry xxx (xxxx) xxx

Contents lists available at ScienceDirect

Analytical Biochemistry

journal homepage: www.elsevier.com/locate/yabio

How many molecules of mitochondrial complex I are in a cell?

Fariha Ansari [a], Belem Yoval [a], Zoya Niatsetskaya [b,c], Vadim Ten [b,c], Ilka Wittig [d,e], Alexander Galkin [a,*]

[a] Feil Family Brain and Mind Research Institute, Weill Cornell Medicine, New York, NY, USA
[b] Department of Pediatrics, Rutgers-Robert Wood Johnson Medical School, New Brunswick, NJ, 08901, USA
[c] Department of Medicine, Rutgers-Robert Wood Johnson Medical School, New Brunswick, NJ, 08901, USA
[d] Functional Proteomics, Institute of Cardiovascular Physiology, Goethe University, 60590, Frankfurt am Main, Germany
[e] German Center for Cardiovascular Research (DZHK), Partner site RheinMain, Frankfurt am Main, Germany

ARTICLE INFO

Keywords:
Mitochondrial complex I
Flavin mononucleotide
Fluorescence
Respiratory chain
Astrocytes

ABSTRACT

Mitochondrial complex I is the only enzyme responsible for oxidation of matrix NADH and regeneration of NAD^+ for catabolism. Nuclear and mtDNA mutations, assembly impairments, and enzyme damage are implicated in inherited diseases, ischemia-reperfusion injury, neurodegeneration, and tumorogenesis.

Here we introduce a novel method to measure the absolute content of complex I. The method is based on flavin fluorescence scanning of a polyacrylamide gel after separation of complexes by Clear Native electrophoresis. Using mouse primary astrocytes as an example, we calculated an average value of 2.2×10^5 complex I molecules/cell. Our method can be used for accurate quantification of complex I content.

1. Introduction

Proton-translocating NADH:ubiquinone oxidoreductase (MT-ND, EC 1.6.5.3) or mitochondrial complex I is one of the largest components of the respiratory chain. Complex I catalyzes oxidation of matrix NADH by ubiquinone, which is coupled with proton translocation across the inner mitochondrial membrane (see Refs. [1,2] for reviews). The hydrophilic domain of the enzyme contains one molecule of flavin mononucleotide (FMN) that directly oxidizes matrix NADH and transfers electrons downstream to FeS clusters [3–8].

Dysfunction at the level of oxidative phosphorylation is a prominent feature in many neurodegenerative diseases, and deficits in complex I may contribute to or even underlie the mitochondrial impairments. Alterations in complex I in highly metabolizing tissues like the brain and heart are linked to multisystemic disorders manifested in early childhood or age-dependent pathologies. Complex I activity is reduced in the brain samples of patients with mtDNA mutations [9,10], Parkinson's disease [11], Friedreich ataxia [12], amyotrophic lateral sclerosis [13], and also cancer [14].

Complex I deficiencies are usually displayed as reduced specific NADH:ubiquinone oxidoreductase activity due to functional impairments and/or post-translational modifications and can also be induced by secondary effects at the level of assembly or mitochondrial morphology, decreasing the absolute content of the enzyme in diseased tissues. Therefore, it is of great importance to know the endogenous mechanism in cells and patient samples: whether it is a drop in catalytic efficiency of the enzyme (turnover number) or a drop in the absolute content of competent complex I.

Rapidly rising interest in clinically-oriented studies of mitochondrial complex I at the level of primary and cultured cells [15–23] requires a fast and reliable procedure for determination of the absolute content of complex I in cells.

The method presented here introduces a novel approach to measure the absolute content of complex I in cultured or primary cells. Using primary cultures of mouse astrocytes, we developed a reliable procedure for the determination of complex I content in a single cell. Our method is based on flavin fluorescence scanning of a polyacrylamide gel after separation of mitochondrial complexes by high resolution Clear Native (hrCN) electrophoresis and denaturation of complex I.

2. Materials and methods

2.1. Reagents

The following chemicals were purchased from Sigma: aminocaproic acid (A2504), DDM (#D4641), Deoxyribonuclease I (#DN25), EDTA

* Corresponding author.
E-mail address: alg2057@med.cornell.edu (A. Galkin).

https://doi.org/10.1016/j.ab.2022.114646
Received 9 December 2021; Received in revised form 1 March 2022; Accepted 4 March 2022
Available online 5 March 2022

(#E-5391), Fetal Bovine Serum (#F4135), FMN (#F2253), imidazole (#792527), NADH (#N8129), PMSF (#P7626), SDS (#L3771), sodium deoxycholate (#D6750), tricine (#T0377), and triphenyl-tetrazolium chloride (#T8877). Cell growth media components DMEM (#10569), GlutaMAX (#10566016), Penicillin-Streptomycin (#15140122) were from Gibco. NativeMark unstained protein standards (#LC0725), Pierce BCA protein assay kit (#23225), and 3–12% polyacrylamide gradient gel, 8 × 8 cm (#BN1001BOX) were from Thermo Fisher Scientific. Difluorocarboxyfluorescein NHS-ester was from Fluoroprobes (#1223).

2.2. Sample preparation, hrCN electrophoresis and fluorescent scanning

Mouse brain cortex primary astrocytes were derived from P0–P2 neonatal mice from dissociating the cerebral cortex based on the procedure described in Ref. [24] with minor modifications [25]. Cells were seeded in poly-D-lysine–coated flasks on a DMEM medium containing GlutaMax (1 ×), 10% FBS, 33 units/mL penicillin, and 33 μg/mL streptomycin. Cells were grown and maintained at 37 °C at atmospheric oxygen levels (20% O2, 5% CO2) in a Binder CB 150-UL CO2 incubator. Sample preparation was essentially based on a previously developed technique [26] with the following modifications. Briefly, flasks were rinsed with PBS, cells were scraped from flasks, washed with PBS at 600 g for 4 min, and counted with trypan blue before the final centrifugation. Protein BCA assay in the presence of 1% deoxycholate yielded 0.4 mg total cellular protein per 10^6 cells.

To solubilize harvested astrocytes, 10^6 cells were resuspended in 70 μL of hypotonic solubilization buffer (10 mM imidazole pH 7, 0.2 mM EDTA, 0.1 M aminocaproic acid, 1 μM $CaCl_2$, 50 μM PMSF, 50 μg DNase) and homogenized in the presence of DDM (2.5 g/g detergent to protein ratio) for 1 min at 1450 rpm in a tightly-fitted Potter homogenizer. Homogenates were then sonified with 3, 1 s pulses at 30% amplitude with the Cole-Parmer 500-Watt Ultrasonic Homogenizer (microtip horn).

For the preparation of homogenates, fresh mouse brain tissue was harvested and suspended in tenfold excess of MSE buffer composed of 225 mM mannitol, 75 mM sucrose, 20 mM HEPES–KOH, 1 mM EGTA, pH 7.4. Samples were homogenized with a Teflon glass Potter homogenizer for 1 min at 1450 rpm. Homogenates were centrifuged at 500 g for 4 min, and the resulting supernatants were pelleted at 10,000 g for 10 min. Tissue homogenates (1 mg) were resuspended in 35 μl solubilization buffer and 2.0 g/g DDM was added. DDM-treated suspensions were centrifuged for 20 min at 20,000 g, and the pellet was discarded.

Samples were supplemented with 0.1% Ponceau S in 50% glycerol and loaded onto a 3–12% polyacrylamide gradient gel. For fast and convenient protein markers detection, commercially available NativeMark unstained protein standards (Thermofisher) were non-specifically labeled with difluorocarboxyfluorescein NHS-ester, so they are clearly visible during flavin fluorescence scanning. Electrophoresis was performed using the Invitrogen XCell SureLock Electrophoresis Cell and the Invitrogen PowerEase 500 Power Supply. Gels were run in the cold (4 °C) with the following conditions: 30 min 30 V, 1 h 60 V, and 3 h 190 V with a limit of 20–30 mA per gel. The cathode buffer was composed of 50 mM Tricine, 7.5 mM imidazole, pH 7.0, 0.01% DDM and 0.05% deoxycholate, and the anode buffer contained 25 mM imidazole/HCl, pH 7.0. Electrophoresis was stopped after the red front reached the bottom. Gels were taken out of the plastic casting plates and analyzed either for complex I in-gel activity [26,27] or scanned for flavin fluorescence.

To detect complex I in-gel activity, the NADH:nitrotetrazolium blue reaction was utilized. Gel strips were placed in 10 ml of 5 mM Tris/HCl, pH 7.4, 0.2 mM EDTA assay buffer supplemented with 2.5 mg/ml of nitrotetrazolium blue and 150 μM NADH. After a 4–6 min incubation at room temperature, the reaction was stopped using the fixing solution (50% methanol, 10% acetic acid).

For flavin fluorescence scanning, the gel was placed in a Typhoon 9000 image scanner (GE) for flavin fluorescence detection using a 473 nm laser for excitation and BPB1 emission filter (530 nm maximum, 20 nm bandpass). The detector voltage was 950 V. To denature complex I, 0.5 ml of 20% SDS solution was applied with a micropipette on the surface of the gel located on the scanner stage. The SDS solution was evenly distributed on the surface of the entire gel and after 15–20 min flavin fluorescence scanning was performed.

Standard FMN solutions were prepared in water and their concentration was measured spectrophotometrically ($\epsilon_{450} = 12.5\ mM^{-1}cm^{-1}$) [5]. Aliquots of the solutions were stored at −20 °C and used only once. After SDS-treatment, 1–3 μL of standard 0.31 and 1.25 μM solutions of FMN were added with a micropipette directly on the surface of the gel and scanned to obtain a signal from the lanes and calibration spots.

2.3. Statistical analysis

In-gel signal intensities from flavin fluorescence scans were analyzed using ImageLab software (version 6, Biorad). The region of interest was placed over the fluorescence band, and the mean intensity was calculated and background subtracted. Data analysis was performed using Microcalc Origin (version 8Pro). All data are mean ± SEM. A two-tailed *t*-test was used to analyze the differences between two groups.

3. Results

3.1. hrCNE of intact brain mitochondria and flavin fluorescence

Primary cultured astrocytes were solubilized with DDM as described in Materials and Methods. We used 1 mg DDM per 10^6 cells, however for different cell cultures pilot testing with lower and higher amounts of detergent is required. Full disassembly of supercomplexes is observed at such a high DDM concentration, and only individual respiratory complexes can be detected [26]. Aliquots containing total solubilized homogenate were applied to a polyacrylamide gradient gel. The location of complex I was identified from the position of molecular weight markers (850 kDa band) and also from in-gel activity (Fig. 1A). Initially, flavin fluorescence scanning (excitation/emission = 473/530 nm) did not show any flavin signal from the complex I band since FMN fluorescence is quenched in the intact enzyme [28–30]. To reveal complex I FMN fluorescence, we used a 20% SDS solution applied directly on the gel surface to denature the apoprotein part. After complete denaturation of the enzyme, FMN fluorescence can be observed (Fig. 1A, lanes 3).

Development of SDS-induced FMN fluorescence, i.e. denaturation of complex I, takes time. Therefore, prior to experiments with cells, we determined the time required for the SDS-induced signal to fully develop using hrCN electrophoresis of DDM-solubilized whole brain homogenates. In our hands, at least 15 min was required for the fluorescence intensity signal to reach its maximum (Fig. 1C-D). Prolonged exposure times resulted in the diffusion of flavin within the polyacrylamide gel and broadening of the band (Fig. 1E).

We calibrated the fluorescence intensity by adding aliquots of free standard FMN solution on the gel (Fig. 1B) and calculated the signal intensity in the spots of the region of interest (Fig. 2A). We were able to measure as little as 15 fmol of flavin, which allowed us to measure FMN when approximately 4×10^4 cells were loaded per well (around 20 μg of protein). However, for practical reasons we used 7-23 × 10^4 cells (Fig. 2A).

In order to plot the dependence of fluorescence intensity upon flavin amount, calibration with standard FMN solutions was performed for each individual gel. As shown in Fig. 2A, the dependence was linear in the range of 0.3–4.0 pmoles FMN with a slope value of $5 \pm 0.04 \times 10^7$ (r value 0.99984, n = 4).

Using a calibration curve in Fig. 2A, we were able to find a dependence between the amount of cells applied and the amount of FMN in the complex I band. From our calibration curves shown in Fig. 2, we calculated that there is 0.93 ± 0.05 pmoles of complex I FMN per mg of total cellular protein or 0.37 ± 0.02 pmoles of complex I FMN per 10^6

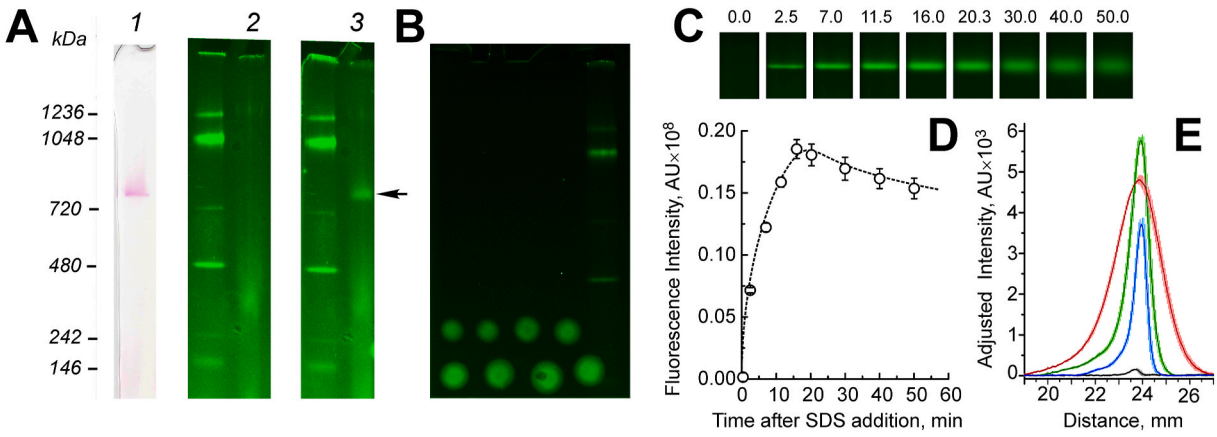

Fig. 1. Separation of DDM-solubilized primary astrocytes by an hrCN gel. A, primary astrocytes were solubilized using a DDM/cell ratio of 1 mg/10^6 cells. Aliquots (23×10^4 cells) were loaded on a polyacrylamide gradient gel (3–12%) and hrCN electrophoresis was performed. **A**, Lane 1 shows complex I in-gel activity. Lanes 2 and 3 show the flavin fluorescence signal (excitation/emission = 473/530 nm) from the same strip before (2) and after (3) 20 min incubation with 20% SDS to denature complex I. The position of complex I is shown by an arrow. Left lanes show the position of difluorocarboxyfluorescein-labeled molecular weight markers in kDa. **B**, flavin fluorescence scan of the part of the gel used for signal calibration. Small aliquots (1–2.5 μL) of standard FMN solution (0.52 μM) were added in duplicates to obtain dependence of the fluorescence intensity upon amount of FMN. FMN amount in each spot from left to right: 0.52, 0.78, 1.04, 1.3 pmoles. **C-E**, kinetics of complex I flavin signal development after 20% SDS was added on the gel surface and repetitive fluorescent scans were performed. DDM-solubilized whole brain homogenate was used, protein load 50 μg **C**, representative scans of flavin fluorescence signal development in complex I band after addition of SDS. Numbers above the gel fragments indicate minutes after SDS addition. **D**, time dependence of the complex I flavin-containing bands' fluorescence intensity change during SDS-treatment. E, densitometric analysis of complex I flavin band intensity appearance and broadening after SDS-addition (black, 0 min, no SDS; blue, 2.5 min; green, 16 min; red, 50 min incubation with SDS). Error bars represent SEM based on quadruplicate measurements. (For interpretation of the references to colour in this figure legend, the reader is referred to the Web version of this article.)

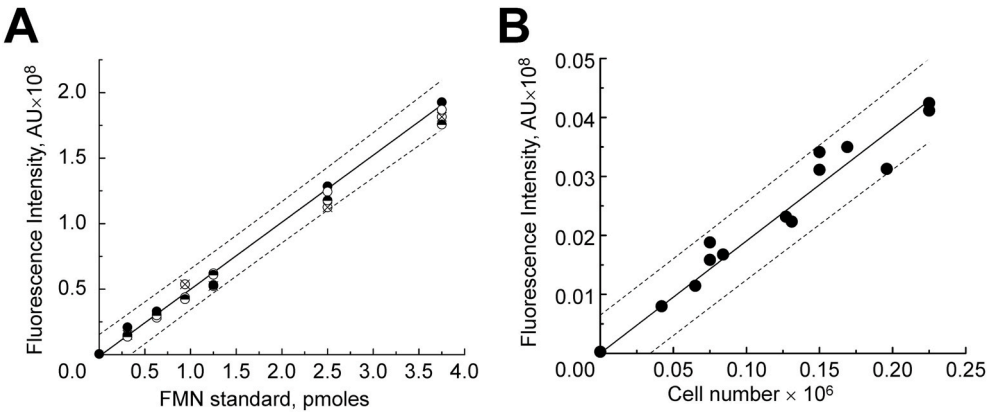

Fig. 2. Properties of flavin fluorescence signal from a hrCN gel of DDM-solubilized primary astrocytes. A, Calibration curve for determination of FMN content in the complex I band made of standard FMN solution applied directly on the gel surface and intensity of fluorescent spots measured as in Fig. 1. Values from four separate calibrations are shown. **B**, Dependence of the fluorescence intensity of complex I bands on cell load on the gel. Values from four different preparations are shown. The solid black line represents the best fit to the data and the dashed lines indicate the 95% confidence interval limits.

cells.

4. Discussion

A considerable amount of published data indicates that impairments in complex I function are involved in the pathophysiology of many neurodegenerative diseases. Due to the complexity of enzyme assembly and maturation processes [21,31–34], changes in specific complex I NADH:ubiquinone enzyme activity measured in patient biopsies or primary fibroblasts may not parallel the alteration of enzyme content in these samples.

Studies of complex I-associated pathologies in primary and cultured cells by measuring only enzyme activity preclude investigation at the cellular level and neglect endogenous factors that may be limiting enzyme activity. The goal of the current study was to develop a method for quantitative measurement of absolute complex I content and relate it to conveniently measured enzyme activity. Our approach was previously validated using mitochondria and tissue homogenates from various sources [27].

Knowledge of the absolute content of complex I in a given sample will permit a quantitative understanding of the fundamental mechanisms underlying enzyme impairment. A quantitative and mechanistic assay may be required for the development of new efficient disease-oriented therapies targeting either impairment of complex I catalytic rate or enzyme altered content.

Our method of complex I detection in cells utilizes first homogenization of the material, solubilization with DDM, separation of mitochondrial complexes by hrCN polyacrylamide gel electrophoresis [26], and flavin fluorescent scanning after denaturation of the enzyme directly in the gel. Clear Native gels are preferable over classic Blue Native polyacrylamide gels [35] because the presence of Coomassie affects the linearity of the fluorescent signal intensity over the utilized protein load. Most likely Coomassie dye interferes with in-gel fluorescence detection, as well as binds at the dinucleotide binding site in enzymes [30,36].

It should also be noted that previously published protocols [26,35,37–39] require isolation of a "crude" mitochondrial fraction, while also discarding the insoluble heavy fraction after membrane solubilization with DDM. In our approach, we homogenize, solubilize, and apply total cellular homogenate on a gel, assuring an accurate estimation of the

number of complex I molecules per amount of starting material.

Complex I flavin fluorescence is quenched upon binding to the protein apoenzyme [28,40–42]. Therefore, no complex I-linked flavin fluorescence was observed in the untreated gel upon the end of electrophoresis. SDS was used as a non-expensive and efficient denaturing agent applied directly on the surface of a gel after separation of native mitochondrial complexes to reveal the flavin fluorescent signal from complex I. SDS-treatment would also allow further separation of complex I subunits by a polyacrylamide gel in denaturing conditions (3D or 2D gels [43]). Long SDS incubation times and multiple scans would result in broadening of the peak and sometimes significant decrease of the signal intensity, probably due to photobleaching. It should be stressed that a shorter incubation time might be required for SDS-induced denaturation when using DDM-solubilized preparations that were frozen and analyzed after thawing. Therefore, we recommend performing a preliminary series of scans in time to determine the optimal interval required for signal detection after SDS addition.

For cultured mouse astrocytes, we obtained a value of 0.93 ± 0.05 pmoles per mg of total cellular protein, which corresponds to 0.37 ± 0.02 pmoles of FMN per 10^6 cells. Therefore, based on Avogadro's number, there are 2.2×10^5 complex I molecules on average in a mouse primary astrocyte. The typical volume of a single astrocyte in situ was determined to be between 40-80 $\times$ 10^3 μm^3 in mice [44]. Therefore, while only localized in mitochondria, the absolute molar intracellular concentration of complex I can be calculated between 5 and 10 nM. This is orders of magnitude lower than the concentration of other enzymes of catabolic pathways such as glycolysis in an average cell (*e.g.*, 1–100 μM for glucose-6-phosphate isomerase) [45–47].

Our method for determination of complex I content complements other approaches for the measurement of the enzyme state. Together with the measurement of conventional specific NADH:ubiquinone activity [27,48–51], our approach would help to calculate catalytic constant values (k_{cat}, moles NADH converted per min) to assess complex I functionality. While this approach can be extremely useful when analyzing the effect of pathological mutations on complex I state, caution must be used in the interpretation of results when flavin-binding subunit NDUFV1 or cellular riboflavin metabolism is expected to be involved.

5. Conclusions

The method described here can be a valuable tool for accurate estimation of absolute complex I content in cultured and primary cells. This information can be extremely useful for the characterization of the complex I state. Due to the role of mitochondrial complex I in human diseases, there is great interest in understanding its regulation and this non-expensive and reliable method will be useful for studying the complex I state in cellular models of inherited or acquired disease or metabolic insults.

CRediT authorship contribution statement

Fariha Ansari: designed the experiments, performed the experiments, Writing – review & editing. **Belem Yoval:** performed the experiments. **Zoya Niatsetskaya:** performed the experiments. **Vadim Ten:** Writing – review & editing. **Ilka Wittig:** designed the experiments, Writing – review & editing. **Alexander Galkin:** designed the experiments, Writing – review & editing, Writing – original draft, wrote the manuscript.

Declaration of competing interest

The authors declare that they have no conflicts of interest with the contents of this article.

Acknowledgments

This work was partially supported by the grants NIH RO1NS112381 (A.G.), NS100850 (V.T.) and by BMBF mitoNET–German Network for Mitochondrial Disorders 01GM1906D (I.W.). We also thank Prof. Eric Green, Department of Biochemistry and Molecular Biophysics Columbia University Medical Center for access to the Typhoon instrument.

References

[1] J. Hirst, Mitochondrial complex I, Annu. Rev. Biochem. 82 (2013) 551–575.
[2] C. Wirth, U. Brandt, C. Hunte, V. Zickermann, Structure and function of mitochondrial complex I, Biochim. Biophys. Acta 1857 (2016) 902–914.
[3] Y. Hatefi, J.S. Rieske, Preparation and properties of DPNH-coenzyme Q reductase (Complex I of the respiratory chain), Methods Enzymol. 10 (1967) 235–239.
[4] C.I. Ragan, The structure and subunit composition of the particulate NADH-ubiquinone reductase of bovine heart mitochondria, Biochem. J. 154 (1976) 295–305.
[5] N. Rao, S.P. Felton, F.M. Huennekens, Quantitative Determination of Mitochondrial Flavins, Methods Enzymol, Academic Press, 1967, pp. 494–499.
[6] G. Belogrudov, Y. Hatefi, Catalytic sector of complex I (NADH:Ubiquinone oxidoreductase): subunit stoichiometry and substrate-induced conformation changes, Biochemistry 33 (1994) 4571–4576.
[7] L.A. Sazanov, P. Hinchliffe, Structure of the hydrophilic domain of respiratory complex I from thermus thermophilus, Science 311 (2006) 1430–1436.
[8] K.R. Vinothkumar, J. Zhu, J. Hirst, Architecture of mammalian respiratory complex I, Nature 515 (2014) 80–84.
[9] M. Zeviani, S. DiDonato, Mitochondrial disorders, Brain 127 (2004) 2153–2172.
[10] K. Fiedorczuk, L.A. Sazanov, Mammalian mitochondrial complex I structure and disease-causing mutations, Trends Cell Biol. 28 (2018) 835–867.
[11] P.M. Keeney, J. Xie, R.A. Capaldi, J.P. Bennett Jr., Parkinson's disease brain mitochondrial complex I has oxidatively damaged subunits and is functionally impaired and misassembled, J. Neurosci. 26 (2006) 5256–5264.
[12] M.H. Salehi, B. Kamalidehghan, M. Houshmand, G. Yong Meng, M. Sadeghizadeh, O. Aryani, S. Nafissi, Gene expression profiling of mitochondrial oxidative phosphorylation (OXPHOS) complex I in Friedreich ataxia (FRDA) patients, PLoS One 9 (2014), e94069.
[13] V. Crugnola, C. Lamperti, V. Lucchini, D. Ronchi, L. Peverelli, A. Prelle, M. Sciacco, A. Bordoni, E. Fassone, F. Fortunato, S. Corti, V. Silani, N. Bresolin, S. Di Mauro, G. P. Comi, M. Moggio, Mitochondrial respiratory chain dysfunction in muscle from patients with amyotrophic lateral sclerosis, Arch. Neurol. 67 (2010) 849–854.
[14] F.A. Urra, F. Munoz, A. Lovy, C. Cardenas, The mitochondrial complex(I)ty of cancer, Front. Oncol. 7 (2017) 118.
[15] A. Baracca, F. Chiaradonna, G. Sgarbi, G. Solaini, L. Alberghina, G. Lenaz, Mitochondrial Complex I decrease is responsible for bioenergetic dysfunction in K-ras transformed cells, Biochim. Biophys. Acta 1797 (2010) 314–323.
[16] E. Fernandez-Vizarra, S. Lopez-Calcerrada, L.E. Formosa, R. Perez-Perez, S. Ding, I. M. Fearnley, J. Arenas, M.A. Martin, M. Zeviani, M.T. Ryan, C. Ugalde, SILAC-based complexome profiling dissects the structural organization of the human respiratory supercomplexes in SCAFI(KO) cells, Biochim. Biophys. Acta Bioenerg. 1862 (2021) 148414.
[17] C. Ugalde, R. Hinttala, S. Timal, R. Smeets, R.J. Rodenburg, J. Uusimaa, L.P. van Heuvel, L.G. Nijtmans, K. Majamaa, J.A. Smeitink, Mutated ND2 impairs mitochondrial complex I assembly and leads to Leigh syndrome, Mol.Genet.Metab 90 (2007) 10–14.
[18] J.A.M. Smeitink, L.W.P.J. van den Heuvel, W.J.H. Koopman, L.G.J. Nijtmans, C. Ugalde, P.H.G.M. Willems, Cell biological consequences of mitochondrial NADH: ubiquinone oxidoreductase deficiency, Curr. Neurovascular Res. 1 (2004) 29–40.
[19] Y. He, K.W. Leung, Y.H. Zhang, S. Duan, X.F. Zhong, R.Z. Jiang, Z. Peng, J. Tombran-Tink, J. Ge, Mitochondrial complex I defect induces ROS release and degeneration in trabecular meshwork cells of POAG patients: protection by antioxidants, Invest. Ophthalmol. Vis. Sci. 49 (2008) 1447–1458.
[20] A. Almeida, M. Delgado-Esteban, J.P. Bolanos, J.M. Medina, Oxygen and glucose deprivation induces mitochondrial dysfunction and oxidative stress in neurones but not in astrocytes in primary culture, J. Neurochem. 81 (2002) 207–217.
[21] D.A. Stroud, E.E. Surgenor, L.E. Formosa, B. Reljic, A.E. Frazier, M.G. Dibley, L. D. Osellame, T. Stait, T.H. Beilharz, D.R. Thorburn, A. Salim, M.T. Ryan, Accessory subunits are integral for assembly and function of human mitochondrial complex I, Nature 538 (2016) 123–126.
[22] R.O. Vogel, C.E. Dieteren, L.P. van den Heuvel, P.H. Willems, J.A. Smeitink, W. J. Koopman, L.G. Nijtmans, Identification of mitochondrial complex I assembly intermediates by tracing tagged NDUFS3 demonstrates the entry point of mitochondrial subunits, J. Biol. Chem. 282 (2007) 7582–7590.
[23] R. Perez-Perez, T. Lobo-Jarne, D. Milenkovic, A. Mourier, A. Bratic, A. Garcia-Bartolome, E. Fernandez-Vizarra, S. Cadenas, A. Delmiro, I. Garcia-Consuegra, J. Arenas, M.A. Martin, N.G. Larsson, C. Ugalde, COX7A2L is a mitochondrial complex III binding protein that stabilizes the III2+IV supercomplex without affecting respirasome formation, Cell Rep. 16 (2016) 2387–2398.
[24] K.D. McCarthy, J. de Vellis, Preparation of separate astroglial and oligodendroglial cell cultures from rat cerebral tissue, J. Cell Biol. 85 (1980) 890–902.

[25] R.W. O'Meara, S.D. Ryan, H. Colognato, R. Kothary, Derivation of enriched oligodendrocyte cultures and oligodendrocyte/neuron myelinating co-cultures from post-natal murine tissues, JoVE 3324 (2011), https://doi.org/10.3791/3324.
[26] I. Wittig, M. Karas, H. Schägger, High resolution clear native electrophoresis for in-gel functional assays and fluorescence studies of membrane protein complexes, Mol. Cell. Proteomics 6 (2007) 1215–1225.
[27] F. Ansari, B. Yoval-Sanchez, Z. Niatsetskaya, S. Sosunov, A. Stepanova, C. Garcia, E. Owusu-Ansah, V. Ten, I. Wittig, A. Galkin, Quantification of NADH:ubiquinone oxidoreductase (complex I) content in biological samples, J. Biol. Chem. 297 (2021) 101204.
[28] W.S. Kunz, W. Kunz, Contribution of different enzymes to flavoprotein fluorescence of isolated rat liver mitochondria, Biochim. Biophys. Acta 841 (1985) 237–246.
[29] I.E. Hassinen, From identification of fluorescent flavoproteins to mitochondrial redox indicators in intact tissues, Journal of Innovative Optical Health Sciences (2014) 1350058, 07.
[30] K. Blinova, R.L. Levine, E.S. Boja, G.L. Griffiths, Z.D. Shi, B. Ruddy, R.S. Balaban, Mitochondrial NADH fluorescence is enhanced by complex I binding, Biochemistry 47 (2008) 9636–9645.
[31] L.E. Formosa, L. Muellner-Wong, B. Reljic, A.J. Sharpe, T.D. Jackson, T.H. Beilharz, D. Stojanovski, M. Lazarou, D.A. Stroud, M.T. Ryan, Dissecting the roles of mitochondrial complex I intermediate assembly complex factors in the biogenesis of complex I, Cell Rep. 31 (2020) 107541.
[32] S. Guerrero-Castillo, F. Baertling, D. Kownatzki, H.J. Wessels, S. Arnold, U. Brandt, L. Nijtmans, The assembly pathway of mitochondrial respiratory chain complex I, Cell Metabol. 25 (2017) 128–139.
[33] B. Pereira, A. Videira, M. Duarte, Novel insights into the role of Neurospora crassa NDUFAF2, an evolutionarily conserved mitochondrial complex I assembly factor, Mol. Cell Biol. 33 (2013) 2623–2634.
[34] C. Ugalde, R. Vogel, R. Huijbens, L. Van den Heuvel, J. Smeitink, L. Nijtmans, Human mitochondrial complex I assembles through the combination of evolutionary conserved modules; a framework to interpret complex I deficiencies, Hum. Mol. Genet. 13 (2004) 659–667.
[35] I. Wittig, H.P. Braun, H. Schägger, Blue native PAGE, Nat. Protoc. 1 (2006) 418–428.
[36] S.T. Thompson, K.H. Cass, E. Stellwagen, Blue dextran-sepharose: an affinity column for the dinucleotide fold in proteins, Proc. Natl. Acad. Sci. U. S. A. 72 (1975) 669–672.
[37] H. Schñgger, G. von Jagow, Blue native electrophoresis for isolation of membrane protein complexes in enzymatically active form, Anal. Biochem. 199 (1991) 223–231.
[38] G. Beutner, G.A. Porter Jr., Native gel electrophoresis and immunoblotting to analyze electron transport chain complexes, Methods Mol. Biol. 2276 (2021) 103–112.
[39] S.M. Nadtochiy, M. Ngai, P.S. Brookes, Modified blue native gel approach for analysis of respiratory supercomplexes, Methods Mol. Biol. 2276 (2021) 227–234.
[40] W.S. Kunz, F.N. Gellerich, Quantification of the content of fluorescent flavoproteins in mitochondria from liver, kidney cortex, skeletal muscle, and brain, Biochem. Med. Metab. Biol. 50 (1993) 103–110.
[41] W.S. Kunz, Spectral properties of fluorescent flavoproteins of isolated rat liver mitochondria, FEBS Lett. 195 (1986) 92–96.
[42] H. Voltti, I.E. Hassinen, Oxidation-reduction midpoint potentials of mitochondrial flavoproteins and their intramitochondrial localization, J. Bioenerg. Biomembr. 10 (1978) 45–58.
[43] I. Rais, M. Karas, H. Schägger, Two-dimensional electrophoresis for the isolation of integral membrane proteins and mass spectrometric identification, Proteomics 4 (2004) 2567–2571.
[44] A. Grosche, J. Grosche, M. Tackenberg, D. Scheller, G. Gerstner, A. Gumprecht, T. Pannicke, P.G. Hirrlinger, U. Wilhelmsson, K. Huttmann, W. Hartig, C. Steinhauser, M. Pekny, A. Reichenbach, Versatile and simple approach to determine astrocyte territories in mouse neocortex and hippocampus, PLoS One 8 (2013), e69143.
[45] D.W. Maughan, J.A. Henkin, J.O. Vigoreaux, Concentrations of glycolytic enzymes and other cytosolic proteins in the diffusible fraction of a vertebrate muscle proteome, Mol. Cell. Proteomics 4 (2005) 1541–1549.
[46] J.R. Wisniewski, A. Gizak, D. Rakus, Integrating proteomics and enzyme kinetics reveals tissue-specific types of the glycolytic and gluconeogenic pathways, J. Proteome Res. 14 (2015) 3263–3273.
[47] K.R. Albe, M.H. Butler, B.E. Wright, Cellular concentrations of enzymes and their substrates, J. Theor. Biol. 143 (1990) 163–195.
[48] M. Spinazzi, A. Casarin, V. Pertegato, L. Salviati, C. Angelini, Assessment of mitochondrial respiratory chain enzymatic activities on tissues and cultured cells, Nat. Protoc. 7 (2012) 1235–1246.
[49] A.J. Janssen, F.J. Trijbels, R.C. Sengers, J.A. Smeitink, L.P. van den Heuvel, L. T. Wintjes, B.J. Stoltenborg-Hogenkamp, R.J. Rodenburg, Spectrophotometric assay for complex I of the respiratory chain in tissue samples and cultured fibroblasts, Clin. Chem. 53 (2007) 729–734.
[50] K. Parey, J. Lasham, D.J. Mills, A. Djurabekova, O. Haapanen, E.G. Yoga, H. Xie, W. Kuhlbrandt, V. Sharma, J. Vonck, V. Zickermann, High-resolution structure and dynamics of mitochondrial complex I-Insights into the proton pumping mechanism, Sci. Adv. 7 (2021), eabj3221.
[51] V.D. Sled, A.D. Vinogradov, Kinetics of the mitochondrial NADH-ubiquinone oxidoreductase interaction with hexammineruthenium(III), Biochim. Biophys. Acta 1141 (1993) 262–268.

List of abbreviations

BSA: bovine serum albumin
DDM: n-dodecyl-β-D-maltoside;
EGTA: ethylene glycol-bis(β-aminoethyl ether)-N,N,N′,N'-tetraacetic acid
FMN: flavin mononucleotide;
hrCN: high resolution Clear Native;
SDS: sodium dodecyl sulfate